Accepted Manuscript

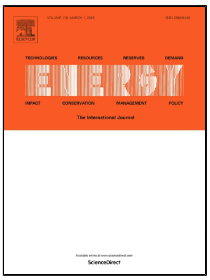

Which dimensional model for the analysis of a coated tube adsorber for adsorption heat pumps?

João M.S. Dias, Vítor A.F. Costa

PII:	S0360-5442(19)30432-3
DOI:	10.1016/j.energy.2019.03.028
Reference:	EGY 14864
To appear in:	*Energy*
Received Date:	21 December 2018
Accepted Date:	06 March 2019

Please cite this article as: João M.S. Dias, Vítor A.F. Costa, Which dimensional model for the analysis of a coated tube adsorber for adsorption heat pumps?, *Energy* (2019), doi: 10.1016/j.energy.2019.03.028

Which dimensional model for the analysis of a coated tube adsorber for adsorption heat pumps?

João M. S. Dias [a,b,*], Vítor A. F. Costa [a,b]

[a] Department of Mechanical Engineering, University of Aveiro, Campus Universitário de Santiago, 3810-193 Aveiro, Portugal

[b] TEMA – Centre for Mechanical Technology and Automation, University of Aveiro, Campus Universitário de Santiago, 3810-193 Aveiro, Portugal

* Corresponding author tel.: +351 234370830; fax: +351 234370830;
web: http://www.ua.pt.

E-mail addresses: joaomdias@ua.pt (J. M. S. Dias); v.costa@ua.pt (V. A. F. Costa)

Abstract

This paper presents the analysis of a coated tube adsorber for adsorption heat pumps (AHP), starting from a well-established physical model and providing information on how many dimensions need to be considered for a given accuracy. A lumped-parameter model, one-dimensional (radial direction) and two-dimensional (radial and longitudinal directions) distributed-parameter models describing the adsorber's dynamics are discussed. The optimal resolution, guaranteeing an accuracy of ≈1% with lower computational efforts is identified. Results obtained with the three dimensional models are compared and their suitability to predict the coefficient of performance (COP) and the specific heating power (SHP) of an AHP is investigated. Results show that the lumped-parameter model is able to predict the COP with minor deviations from the reference model; however, the SHP is overestimated. Furthermore, several sensibility analyses are performed aiming to assess the influence of important parameters, such as the adsorber tube length and heat transfer fluid's (HTF) velocity. In addition, the influence of disregarding the adsorber metal tube mass is evaluated, resulting in deviations up to ≈4.5% for the COP and ≈7% for the SHP, which are considered significant. Results guide researchers to adopt a given dimensional model for the required accuracy.

Keywords

Dimensional models; adsorption heat pump; adsorber; coated tube; coefficient of performance (COP); specific heating power (SHP)

Contents

Nomenclature

C	Specific heat (J/kg.K)
C_p	Constant pressure specific heat (J/kg.K)
d	Diameter (m)
D_{ef0}	Effective diffusivity coefficient (m^2.s)
E_a	Activation energy ($J.kg^{-1}$)
H	Enthalpy (J)
$h_{f\rightarrow m}$	Convective heat transfer coefficient between fluid and metal ($W.K^{-1}.m^{-2}$)
$h_{m\rightarrow s}$	Heat transfer coefficient between metal and adsorbent ($W.K^{-1}.m^{-2}$)
k	Thermal conductivity ($W.K^{-1}.m^{-1}$)
k_0	Pre-exponential coefficient ($kg.kg^{-1}.Pa^{-1}$)
k_D	Blake-Kozeny coefficient (m^2)
K_{LDF}	LDF constant (s^{-1})
L	Tube length (m)
m	Mass (kg)
P	Pressure (Pa)
Q	Heat (J)
q_m	Monolayer capacity ($kg.kg^{-1}$)
r	Radial coordinate (m)
R'	Particular gas constant ($J.kg^{-1}K^{-1}$)
t	Time (s)
t_{SG}	Non-dimensional Toth constant
T	Temperature (K)
u	Heat transfer fluid velocity ($m.s^{-1}$)
X	Adsorbate concentration in the adsorbent ($kg_a.kg_s^{-1}$)
z	Axial coordinate (m)

Subscripts

a	Adsorbate
ads	Adsorption
bed	Adsorbent bed
c	Condenser /Cooling
cyc	Cycle
e	Evaporator
eq	Equilibrium
f	Fluid
h	Heating
ic	Isosteric cooling
ih	Isosteric heating
m	Metal
p	Particle
reg	Regeneration
s	Adsorbent
v	Vapor/Vaporization

Greek letters

ΔH_{ads}	Heat of adsorption ($J.kg^{-1}$)
ε	Porosity
μ	Dynamic viscosity (Pa.s)
σ	Thickness (m)
τ	Cycle time (s)

1. Introduction

Heating and cooling is the biggest energy sector in Europe, accounting for 50% of the total energy consumption much of it being wasted. Renewable energies only account for 18% of the total energy used for heating and cooling, to which the most contributions come from fossil fuels (75%) and a tiny part from nuclear sources (7%) [1]. Therefore, there is a need for heating/cooling systems driven by renewable energy sources in order to mitigate resources consumption and global warming. Adsorption cooling has been the focus over the last decades with several units for air conditioning, refrigeration and chillers being developed. However, adsorption heating is still at its initial stage [2]. Adsorption heat pumps (AHPs) can provide heat and are a potential viable alternative to the conventional vapor compression heat pumps (VCHPs), which use CFCs, HCFCs and other high global warming potential (GWP) substances, even if important changes are running towards the use of natural refrigerants. AHPs have low environmental impact since they use zero or nearly zero GWP operating substances, significantly contributing to decrease the greenhouse gases emissions [3]. The fact that they can be driven by natural gas [3], waste heat [4,5] and renewable energy sources like solar energy [6–8] gives the technology great potential. In addition, electricity can also be used to drive the system and when/if it is obtained from renewable energy sources, the heating system is considered renewable as well [9].

Heat pumps extract heat from a low temperature level and deliver it at an intermediate temperature level, as long as a third energy source is provided [10]. AHPs are driven by higher temperature energy sources that can provide heat to the system, for example, waste heat, gas burners, electricity, geothermal and solar energy. A simple AHP can be built by packing or coating an adsorbent material on a heat exchanger (HEx), a condenser, an expansion valve, an evaporator and a heat transfer system (HTS) or fluid (HTF) to collect/deliver heat from/to the adsorber. Four main configurations for the adsorber can be identified, namely loose grain, consolidated adsorbent, in situ crystalized coatings and binder-based coatings [11]. A detailed overview on the AHPs technology can be found in literature [12]. The energy scheme of a common AHP system is presented in Fig. 1.

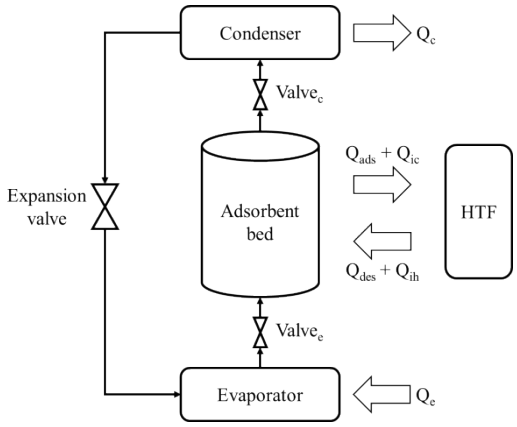

Fig. 1 – Energy scheme of a common adsorption heat pump [12].

The majority of studies found in literature focus on the adsorbent materials, adsorbers' designing or operating conditions. Comparisons between different dimensional models for the same conditions as well as parametric sensibility studies for the physical models are lacking. Information about the effects of using the same physical models for different system parameters and dimensional models (0D, 1D and 2D) is needed to guide researchers to adopt a given dimensional model for the required accuracy, and mainly to achieve accurate performance predictions. This particular information cannot be found in literature, which forces researchers to perform several sensibility and dimensional analyses before achieving the desired accuracy, wasting lots of time and effort. This paper presents some dimensional and sensibility analyses to well-established AHP's physical models, quantifying their computational cost and accuracy for the system's performance predictions.

Several physical models aiming to describe the adsorber of an AHP system can be found in literature. A comprehensive and detailed review on physical and numerical models for AHPs was presented by Pesaran *et al.* [13]. The models can be divided in three types: thermodynamic models, lumped-parameter models and distributed-parameter models. Thermodynamic models disregard heat and mass transfer kinetics inside the adsorber, assuming thermodynamic equilibrium between the adsorbent and adsorbate. This type of models can be used to estimate the upper limits of the system's performance. Lumped-parameter models consider heat and mass transfer to/from the adsorber, assuming that the entire adsorber is in thermodynamic equilibrium and at uniform pressure and temperature. Although some models consider the LDF model to account for the internal mass transfer resistance [14], external mass transfer resistance is neglected. These kind of models are more accurate than thermodynamic models. Distributed-parameter models are the most accurate ones, considering internal and external mass and heat transfer resistances, and pressure and temperature

gradients inside the adsorber. These models are more computationally expensive but, given the recent easy access to powerful computers, they have become more appealing [13]. Computational simulation tools like MATLAB R2017b (Massachusetts, USA), MODELICA (Linköping, Sweden) and computational fluid dynamics (CFD) software have recently been used to perform simulations of AHPs [4,15,16].

Given their high thermal conductivities, higher adsorbent-metal heat transfer coefficients and compact sizes, coated tube adsorbers are nowadays considered the best configuration for AHPs by many researchers [12]. Frazzica *et al.* [17] performed an experimental characterization of a binder-based coating composed of SAPO-34 as adsorbent and a clay as binder. The experiments were conducted based on the large pressure jump (LPJ) method. The coatings were compared to two loose adsorbent grain configurations, one monolayer and one multilayer. Several coating thicknesses were tested and evaluation based on the volumetric specific cooling power (VSCP). Although the loose grain monolayer showed better kinetic performance, the 0.6 mm thick coating showed an increasing in the VSCP of 65% relatively to the monolayer loose grain. Freni *et al.* [18] also studied the adsorption kinetics of a SAPO-34 based adsorbent coating. They concluded that the binder did not affect the adsorption capacity, and that the mass specific cooling power was greatly improved. However, the VSCP was better for the granular adsorbent. In addition, the stability of the adsorbent coating was also tested for 600 adsorption cycles without degradation of the adsorption capacity. SAPO-34 coatings were also used by Wittstadt *et al.* [19] and a COP of 1.4 was reported for heating applications. The effect of the binder used to form the adsorbent coatings on their adsorption capacity was also investigated by Calabrese *et al.* [20]. They characterized three silane binder based coatings, and verified that the adsorption capacity of the three adsorbents was not affected by the binders.

Given that adsorbent coatings provide a very promising solution for adsorption heating solutions, three dynamic models for a coated tube adsorber were considered with different dimensions, namely a lumped-parameter model, a one-dimensional (radial direction) distributed-parameter model and a two-dimensional (radial and longitudinal directions) distributed-parameter model. The considered models take into consideration results reported in literature [21–23] and were adapted and improved for a specific adsorber module design for central and domestic water heating.

Although there are several studies on numerical models for AHPs, and it is guaranteed that lumped-parameter models are less accurate than distributed-parameter ones, it is important to quantify their accuracy differences and computational costs. Only then, researchers can make sustained decisions on

which dimensional model should be used considering their desired accuracy and acceptable computational effort. In addition, it is intrinsic to physical models that the more dimensions are considered the better the accuracy will be; but how much? Is the improvement in the model's accuracy worth the additional computational cost? In order to answer these questions it is necessary to quantify the accuracy improvement associated to the consideration of additional spatial dimensions and the associated computational effort and time. Comparisons of different dimensional models based on the same parameters and considerations (which is required to draw useful conclusions) cannot be found in literature. The identification of the best dimensional model (balance between complexity and computational cost versus accuracy) for a particular application can be performed based on the results from this paper, saving a lot of time and effort to those that need to design an AHP system. Thus, decisions can be taken on the necessity of considering all three spatial dimensions or if a lumped-parameter, a one-dimensional or a two-dimensional model is enough to achieve the desired accuracy. In the following sections, different dimensional models for a coated tube adsorber module are presented and discussed. The objective is to analyze the performance of the different dimensional models quantifying the deviations from the most accurate solution. The influence of some parameters on the deviations of the different dimensional models is investigated.

This work focuses on the dimensional models analysis and not on the adsorber characterization itself, aiming to help researchers decide which dimensional model needs to be considered to achieve the desired accuracy. The common lumped-parameter (0D) and distributed-parameter approaches (1D and 2D) are investigated and their main differences quantified. Furthermore, the effects of considering different dimensional models when evaluating the AHP's performance parameters are evaluated and reported. Several comparisons and sensibility analyses of the dimensional models' accuracy to the change of several parameters like the tube length, heat transfer fluid velocity and metal mass are also carried out. Results presented in this paper can be used to decide which dimensional model needs to be considered and which simplifications can be assumed while still guaranteeing a desired accuracy level. Thus, better agreement between numerical simulations and experimental results can be expected, leading to improved prototype design and faster final application development.

Finally, the adsorber's metal mass is usually disregarded in many studies found in literature [22–24]. The quantification of the deviations caused by disregarding that metal mass cannot be found in the literature. It is important to know how much the accuracy is compromised when the metal mass is neglected in order to decide if it is important or not to consider it for each particular

application. Therefore, the effects of the adsorber's metal mass are also investigated in this paper, quantifying the deviations on the system's performance predictions when it is not taken into account.

2. AHP's dimensional models

The binder-based coated-tube adsorber module represented in **Fig. 2**a was designed, which is considered the best hypothesis for a practical adsorber to integrate an AHP system. It is composed by metal tubes externally coated by adsorbent material and by two joints connecting them. For a simpler and clearer visualization, in Fig. 2 not all the holes of the joints are connected to the correspondent externally coated metal tubes. The joints are linked to the inlet/outlet through which the heat transfer fluid flows, circulating in the interior of the externally coated tubes. The entire component is embedded in a vacuum chamber with connections to the evaporator and condenser, as represented in Fig. 2b.

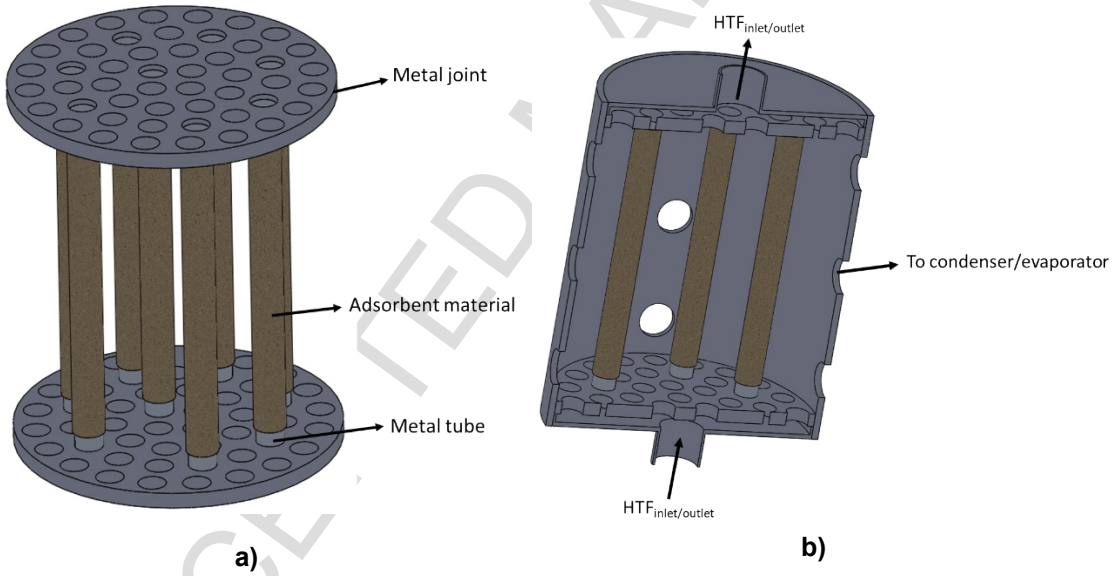

Fig. 2 – a) Adsorber module containing several metal tubes with an external adsorbent material coating; b) Adsorber module cross section view.

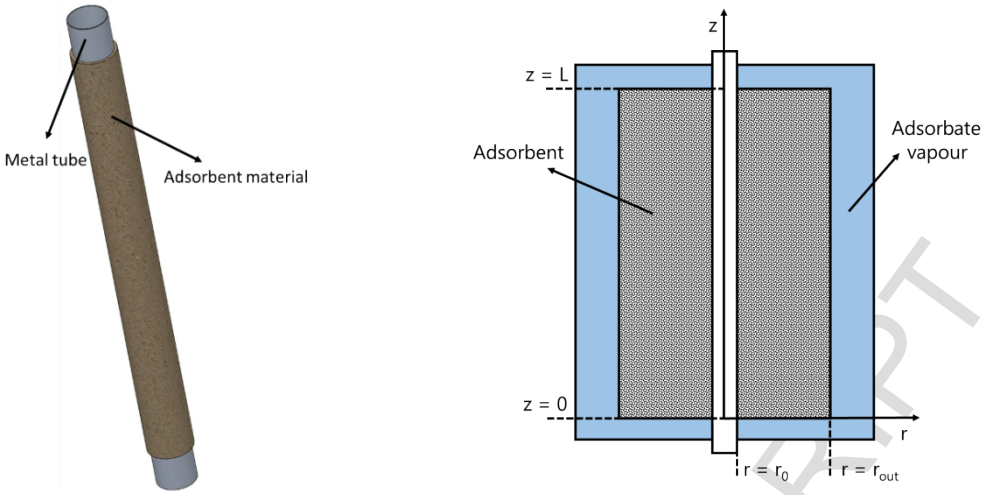

Fig. 3 – Representative element for the development of the physical models (on the left) and schematics (on the right) [12].

The implemented dimensional models are adapted from Zhang *et al.* [22] in order to describe the adsorber's behavior. The model was experimentally validated for the zeolite 13X-water pair by Zhang *et al.* [22] for an adsorption cooling unit, considering the three space dimensions. Since the adsorber contemplated in this work is symmetric along the angular direction for each coated tube, a 2D model is enough to completely describe the adsorber.

All the considered dimensional models describe the dynamics of the representative element from Fig. 3 to achieve useful comparisons between them. The selected adsorbent-adsorbate working pair is silica gel RD-water since it is well studied and its thermo-physical properties can easily be found in literature. Several applications of the silica gel-water pair for adsorption heat transformation as well as its adsorption isotherms and thermophysical properties are described and experimentally characterized in [25–30], which are assumed as the experimental validation of the silica gel-water adsorption kinetics. Considering the aforementioned experimental validations of the model itself and the adsorption kinetics for the silica gel-water pair, the 2D model provides trustworthy results for the dimensional models' analysis, which is the objective of this work. However, all the dimensional models are prepared to work with all working pairs that can be described by the LDF model, as long as their equilibrium isotherms and diffusion coefficients are available. Although the use of a binder to apply the coating affects the adsorber's performance, its effect was neglected since the objective is to compare the different dimensional models and not to characterize the adsorber itself. The dimensional models are different spatial implementations of the energy and mass conservation equations, Equations (1) and **Error! Reference source not found.**, respectively, for the selected design.

$$\frac{\partial(\rho C_p T_s)}{\partial t} + \nabla(\rho_v C_{p,v} T_s u) - \nabla(k_s \nabla T_s) - \rho_s(1-\varepsilon)\Delta H_{ads}\frac{\partial X}{\partial t} = 0 \quad (1)$$

$$\varepsilon\frac{\partial \rho_v}{\partial t} + \nabla(\rho_v u) + \rho_s(1-\varepsilon)\frac{\partial X}{\partial t} = 0 \quad (2)$$

with,

$$\rho C_p = \varepsilon\rho_v C_{p,v} + \rho_s(1-\varepsilon)(C_s + XC_{p,a}) \quad (3)$$

and

$$\varepsilon = \varepsilon_{bed} + (1-\varepsilon_{bed})\varepsilon_p \quad (4)$$

The momentum balance is described by the Darcy's Law (5), and the adsorbent bed permeability is calculated by using the Blake-Kozeny model (6) [31]:

$$u = -\frac{k_D}{\mu}\nabla P \quad (5)$$

where,

$$k_D = \frac{d_p^2 \varepsilon_{bed}^3}{150(1-\varepsilon_{bed})^2} \quad (6)$$

The uptake is described by the linear driving force model (LDF) [14]:

$$\frac{dX}{dt} = K_{LDF}(X_{eq} - X) \quad (7)$$

The K_{LDF} constant is a function of temperature and is calculated by [32]:

$$K_{LDF} = \frac{15 D_{ef0} e^{-\frac{E_a}{R' T_s}}}{R_p^2} \quad (8)$$

For the silica gel RD-water working pair X_{eq} can be obtained by [27]:

$$X_{eq} = \frac{P k_0 e^{\frac{\Delta H_{ads}}{R' T_s}}}{\left[1 + \left(\frac{P k_0}{q_m} e^{\frac{\Delta H_{ads}}{R' T_s}}\right)^{t_{SG}}\right]^{\frac{1}{t_{SG}}}} \quad (9)$$

2.1. General assumptions

The following set of assumptions was considered for all dimensional models considered:

- Adsorbent bed is homogenous;
- The evaporator and the condenser are ideal heat exchangers with uniform pressures;
- Adsorbate vapor phase behaves as an ideal gas and the adsorbed phase is considered to be liquid;
- Specific heats for the adsorbate vapor and liquid phases are constants;
- Adsorbate vapor around the adsorbent is always in the saturated conditions;
- Thermophysical properties of solid materials do not change with temperature;
- The pre-heating and pre-cooling phases are terminated when the pressure in the adsorber reaches the condenser and evaporator pressures, respectively.

2.2. Lumped parameter model (0D model)

The lumped parameter model results from the mass and energy conservation equations applied to the representative element of the adsorber, under the following additional assumptions:

- Temperature and pressure are uniform in the adsorbent bed;
- Adsorbate is uniformly adsorbed and desorbed by the adsorbent;
- The uptake is constant during pre-heating (isosteric heating) and pre-cooling (isosteric cooling) phases.

The uptake is described by:

$$\frac{dX}{dt} = K_{LDF}(X_{eq} - X)(\alpha), \tag{10}$$

$$\begin{cases} Isosteric\ phases & \rightarrow \alpha = 0 \\ Adsorption/Desorption & \rightarrow \alpha = 1 \end{cases}$$

The adsorbent bed energy balance equation is given by:

$$[\rho_s(1-\varepsilon)(C_s + XC_{p,a}) + \varepsilon\rho_v C_{p,v}]\frac{dT_s}{dt} == (1-\varepsilon)\rho_s \Delta H_{ads}\frac{dX}{dt} + \frac{4d_{out,tube}h_{m\to s}(T_m - T_s)}{d_{out,s}^2 - d_{in,s}^2} \quad (11)$$

with $d_{in,s} = d_{out,tube}$.

The differential form of the ideal gas law describes the adsorbent bed mass balance:

$$\frac{d\rho_v}{dt} = \frac{P}{T_s^2 R'}\left(-\frac{dT_s}{dt}\right)(\gamma) + \frac{1}{R' T_s^2}\left(T_s\frac{dP}{dt} - \rho_v\frac{dT_s}{dt}\right)(\delta) \quad (12)$$

$$\begin{cases} Isosteric\ phases & \to \gamma = 0,\ \delta = 1 \\ Adsorption/Desorption & \to \gamma = 1,\ \delta = 0 \end{cases}$$

The adsorbent bed pressure is obtained from the Clausius-Clapeyron equation [33], which can be rearranged as:

$$\frac{dP}{dt} = \frac{PL_v}{R' T_s^2}\left(\frac{dT_s}{dt}\right)(\beta) \quad (13)$$

$$\begin{cases} Isosteric\ phases & \to \beta = 1 \\ Adsorption/Desorption & \to \beta = 0 \end{cases}$$

The pressure variation with time is considered to be null during adsorption and desorption phases because these processes are considered to be isobaric, at the evaporator and condenser pressures, respectively.

Lastly, the metal tube energy balance equation is:

$$\rho_m C_m \frac{dT_m}{dt} = \frac{4d_{in}h_{f\to m}(T_f - T_m)}{d_{out}^2 - d_{in}^2} + \frac{4d_{out}h_{m\to s}(T_s - T_m)}{d_{out}^2 - d_{in}^2} \quad (14)$$

$$\begin{cases} Adsorption/Isosteric\ cooling & \to T_f = T_{ads} \\ Desorption/Isosteric\ heating & \to T_f = T_{reg} \end{cases}$$

For laminar flow conditions ($Re_f \leq 2300$) of the heat transfer fluid inside the adsorber tubes the Nusselt number is obtained considering the constant heat flux situation [34]:

$$Nu_f = 4.36 \quad (15)$$

For $2300 < Re_f \leq 5 \times 10^6$ and $0.5 \leq Pr \leq 2000$ the Nusselt number is obtained through the Gnielinsky correlation [35] (caution should be taken when using this correlation for $Re_f < 3000$):

$$Nu_f = \frac{\left(f/8\right)(Re_f - 1000)Pr}{1 + 12.7\left(f/8\right)^{1/2}\left(Pr^{2/3} - 1\right)} \quad (16)$$

where f is calculated using the correlation developed by Petukhov [36]:

$$f = \left(0.79ln(Re_f) - 1.64\right)^{-2} \quad (17)$$

The convective heat transfer coefficient between the fluid and the metal tube is obtained as:

$$h_{f\to m} = \frac{Nu_f k_f}{d_{in}} \quad (18)$$

The set of initial conditions is:

$t_{ini} = 0$ $\qquad$ $P(t_{ini}) = P_{ini}$

$T_m(t_{ini}) = T_s(t_{ini}) = T_{ini}$ $\qquad$ $X(t_{ini}) = X_{eq}$

The differential equations system was solved numerically in MATLAB R2017b (Massachusetts, USA).

2.3. 1D distributed parameter model (radial)

The 1D distributed parameter model was developed considering the following additional assumption:

- Temperature and pressure in the adsorbent bed are uniform over the longitudinal and angular directions;

The uptake is obtained similarly to the lumped parameter model; however, it is now function of the radial coordinate since $T_s(r)$ and $P(r)$ are considered instead. In addition, the uptake is no longer constant during the pre-heating/cooling phases and it is described by Equation (7). The adsorbent bed energy balance equation is given by:

$$\left[\rho_s(1-\varepsilon)(C_s+XC_l)+\varepsilon\rho_v C_{pv}\right]\frac{dT_s}{dt} == (1-\varepsilon)\rho_s\Delta H_{ads}\frac{dX}{dt}+\frac{k_s}{r}\left(\frac{\partial T_s}{\partial r}+r\frac{\partial^2 T_s}{\partial r^2}\right)-\frac{C_{pv}}{r}\left(\rho_v T_s u+rT_s u\frac{\partial\rho_v}{\partial r}+r\rho_v u\frac{\partial T_s}{\partial r}+r\rho_v T_s\frac{\partial u}{\partial r}\right) \quad (19)$$

The mass conservation equation is:

$$\frac{\partial\rho_v}{\partial t}=-\frac{1}{\varepsilon}\left[\rho_s(1-\varepsilon)\Delta H_{ads}\frac{\partial X}{\partial t}+\frac{1}{r}\left(ru\frac{\partial\rho_v}{\partial r}+\rho_v r\frac{\partial u}{\partial r}+\rho_v u\right)\right] \quad (20)$$

The metal tube thermal energy balance equation is equal to its lumped parameter version because the approximation $\frac{\partial T_m}{\partial r}\approx 0$ is considered, since $k_m \gg k_s$. In addition, the temperature of the heat transfer fluid is considered constant along the radial direction, $\frac{\partial T_f}{\partial r}\approx 0$, assuming that $L_{tube} \gg r_{tube}$.
The initial conditions are:

$$t_{ini}=0 \qquad P(t_{ini})=P_{ini}$$
$$T_m(t_{ini})=T_s(t_{ini})=T_{ini} \qquad X(t_{ini})=X_{eq}$$

During the pre-heating/pre-cooling phases, the pressure in the chamber is considered to be equal to the pressure of the external layer of the adsorbent ($P_{chamber}=P_{r=r_{out}}$) within each time step. The boundary conditions for the pressure are:

$$\left.\frac{\partial P}{\partial r}\right|_{r=r_0}=0$$

$$\begin{cases} P|_{r=r_{out}}=P_e, & Adsorption \\ P|_{r=r_{out}}=P_c, & Regeneration \\ \left.\dfrac{\partial P}{\partial r}\right|_{r=r_{out}}=0, & Cooling/Heating \end{cases}$$

For the temperature, the following boundary conditions apply:

$$-k_s\left.\frac{\partial T_s}{\partial r}\right|_{r=r_0}=h_{m\to s}(T_m-T_s)$$

$$\left.\frac{\partial T_s}{\partial r}\right|_{r=r_{out}} = 0$$

In order to solve the physical model's partial differential equations, the method of lines was implemented and the spatial derivatives in the radial coordinate were discretized through the finite difference method. For the first order derivatives, the forward finite difference scheme was used whereas for the second order derivatives, the centered finite difference scheme was implemented. As a result, the partial differential equations were reduced to an ODE system that was solved using MATLAB R2017b (Massachusetts, USA).

2.4. 2D distributed parameter model (radial and longitudinal)

The two dimensional distributed parameter model considers the same assumptions as the one-dimensional model, except for the temperature and pressure that will additionally change along the axial (longitudinal) coordinate. Furthermore, the temperature of the heat transfer fluid will depend on the axial coordinate as well. The uptake is also described by the LDF model and it depends on the axial and radial positions through the variables $T_s(r,z)$ and $P(r,z)$. The adsorbent bed energy balance equation in this case is:

$$\begin{aligned}[\rho_s(1-\varepsilon)(C_s + XC_l) + \varepsilon\rho_v C_{pv}]\frac{dT_s}{dt} \\ == (1-\varepsilon)\rho_s \Delta H_{ads}\frac{dX}{dt} + \frac{k_s}{r}\left(\frac{\partial T_s}{\partial r} + r\frac{\partial^2 T_s}{\partial r^2}\right) - \frac{C_{pv}}{r} \\ \left(\rho_v T_s u_r + rT_s u_r \frac{\partial \rho_v}{\partial r} + r\rho_v u_r \frac{\partial T_s}{\partial r} + r\rho_v T_s \frac{\partial u_r}{\partial r}\right) - C_{pv}\left(T_s u_z \frac{\partial \rho_v}{\partial z} + \right. \\ \left. + \rho_v u_z \frac{\partial T_s}{\partial z}\right) + k_s\left(\frac{\partial^2 T_s}{\partial z^2}\right)\end{aligned} \quad (21)$$

The mass conservation equation is given by:

$$\frac{\partial \rho_v}{\partial t} = -\frac{1}{\varepsilon}\left[\rho_s(1-\varepsilon)\Delta H_{ads}\frac{\partial X}{\partial t} + \frac{1}{r}\left(ru_r\frac{\partial \rho_v}{\partial r} + \rho_v r\frac{\partial u_r}{\partial r} + \rho_v u_r\right) + \rho_v\frac{\partial u_z}{\partial z} + u_z\frac{\partial \rho}{\partial} \right. \quad (22)$$

For the heat transfer fluid, $\frac{\partial T_f}{\partial r} \approx 0$ is assumed since $r_{tube} \ll L_{tube}$ and the fluid velocity, u_f, is constant. The energy balance equation for the heat transfer fluid is given by:

$$\rho_f C_{p,f} \frac{\partial T_f}{\partial t} = k_f \left(\frac{\partial^2 T_f}{\partial z^2} \right) - u_f \rho_f C_{p,f} \frac{\partial T_f}{\partial z} + \frac{4 h_{f \to m}}{d_{in}} (T_m - T_f) \tag{23}$$

For the metal tube $\frac{\partial T_m}{\partial r} \approx 0$ is also assumed and its energy balance equation is:

$$\rho_m C_m \frac{dT_m}{dt} = k_m \left(\frac{\partial^2 T_m}{\partial z^2} \right) + \frac{4 d_{in} h_{f \to m} (T_f - T_m)}{d_{out}^2 - d_{in}^2} + \frac{4 d_{out} h_{m \to s} (T_s - T_m)}{d_{out}^2 - d_{in}^2} \tag{24}$$

The initial conditions are:

$$t_{ini} = 0 \qquad P(t_{ini}) = P_{ini}$$
$$T_m(t_{ini}) = T_f(t_{ini}) = T_s(t_{ini}) = T_{ini} \qquad X(t_{ini}) = X_{eq}(P_{ini}, T_{s_{ini}})$$

During the pre-heating/pre-cooling phases, the pressure in the chamber is considered to be equal to the pressure of the external layer of the adsorbent ($P_{chamber} = P_{r = r_{out}}$) within each time step. The pressure and temperature boundary conditions that define the selected design for the adsorber are:

$$\left. \frac{\partial P}{\partial r} \right|_{r = r_0} = 0$$

$$P|_{r = r_{out}} = P|_{z = 0} = P|_{z = L} = P_e, \qquad Adsorption$$

$$P|_{r = r_{out}} = P|_{z = 0} = P|_{z = L} = P_c, \qquad Regeneration$$

$$\left. \frac{\partial P}{\partial r} \right|_{r = r_{out}} = \left. \frac{\partial P}{\partial r} \right|_{z = 0} = \left. \frac{\partial P}{\partial r} \right|_{z = L} = 0, \qquad Cooling/Heating$$

$$- k_s \left. \frac{\partial T_s}{\partial r} \right|_{r = r_0} = h_{m \to s} (T_m - T_s)$$

$$\left. \frac{\partial T_s}{\partial r} \right|_{r = r_{out}} = \left. \frac{\partial T_s}{\partial z} \right|_{z = 0} = \left. \frac{\partial T_s}{\partial z} \right|_{z = L} = 0$$

$$T_f|_{z=0} = T_{ads}, \qquad Adsorption/Cooling$$

$$T_f|_{z=0} = T_{reg}, \qquad Regeneration/Heating$$

$$\left.\frac{\partial T_f}{\partial z}\right|_{z=L} = 0$$

$$\left.\frac{\partial T_m}{\partial z}\right|_{z=0} = \left.\frac{\partial T_m}{\partial z}\right|_{z=L} = 0$$

In order to solve the physical model's partial differential equations, the method of lines was also implemented and the derivatives in the radial and axial coordinates discretized through the finite difference method. The discretization is performed for the axial coordinate first and then, every element is discretized along the radial coordinate. As for the 1D model, the forward finite difference and the centered finite difference schemes were used for the first and second order derivatives, respectively. As a result, the partial differential equations were reduced to an ODE system and solved using MATLAB R2017b (Massachusetts, USA).

3. Comparison and sensibility analysis of the dimensional models

Results obtained with the three different dimensional models were compared in order to quantify their main differences. The parameters used for the accuracy comparisons are the performance coefficients for heating applications, namely the coefficient of performance (COP) and the specific heating power (SHP), obtained respectively as [12],

$$COP = \frac{Q_c + Q_{4-1} + Q_{1-2}}{Q_{2-3} + Q_{3-4}}, \tag{25}$$

$$SHP = \frac{Q_c + Q_{4-1} + Q_{1-2}}{m_s \tau_{cyc}}, \tag{26}$$

Q_c enters the numerators of Equations (25) and (26) as it is assumed to be useful heat for heating applications. The adsorption (1-2), pre-heating (2-3), regeneration (3-4) and pre-cooling (4-1) heats were calculated as follows [12]:

$$-Q_{1-2} \approx \int_{T_1}^{T_2} [m_s(C_s + XC_{p,a}) + m_m C_m] dT - \int_{X_{min}}^{X_{max}} m_s \Delta H_{ads} dX \quad (27)$$

$$Q_{2-3} \approx \int_{T_2}^{T_3} [m_s(C_s + X_{max} C_{p,a}) + m_m C_m] dT \quad (28)$$

$$Q_{3-4} \approx \int_{T_3}^{T_4} [m_s(C_s + XC_{p,a}) + m_m C_m] dT - \int_{X_{max}}^{X_{min}} m_s \Delta H_{ads} dX \quad (29)$$

$$-Q_{4-1} \approx \int_{T_4}^{T_1} [m_s(C_s + X_{min} C_{p,a}) + m_m C_m] dT \quad (30)$$

$$Q_c = m_s \Delta X \Delta H_v \quad (31)$$

The different dimensional models' results are compared to the most accurate model results, which is the 2D distributed-parameter model with the highest spatial resolution. The selected values for the radial and longitudinal spatial resolutions for the highest accuracy model were $\Delta r = 4 \times 10^{-5}\, m$ and $\Delta z = 2.08 \times 10^{-2}\, m$, respectively. Further decreasing of these space steps results in improvements of less than 1 % for the COP and SHP values, which was found unnecessary for the given purposes.

3.1. Reference parameters

First, a simple analysis was carried out in order to compare the COP and SHP values obtained by each dimensional model, considering the same parameters for all three models. In Table 1 are listed some parameters used in the simulations. These parameters values were taken from several studies available in the literature [25–27,37,38]. A modest heat transfer coefficient between the metal tube and the adsorbent material was considered, since the objective is to investigate the dimensional models and not the optimization of the adsorber's performance. However, it must be mentioned that higher heat transfer coefficients for adsorbent coatings can be found in literature [23].

Table 1 – Standard parameters used in the simulations.

Symbol name	Value	Unit
C_m	910	$J.kg^{-1}.K^{-1}$
C_s	921	$J.kg^{-1}.K^{-1}$
d_p	3.5×10^{-4}	m
$d_{in,tube}$	0.02	m

E_a	2.3314×10^6	J.kg^{-1}
$h_{m \to s}$	100	W.m^{-2}.K^{-1}
k_0	7.3×10^{-13}	kg.kg^{-1}.Pa^{-1}
k_f	0.6	W.m^{-1}.K^{-1}
k_m	205	W.m^{-1}.K^{-1}
k_s	0.198	W.m^{-1}.K^{-1}
L_{tube}	1	m
L_v	2.4×10^6	J.kg^{-1}
q_m	0.45	kg.kg^{-1}
t_{ads}	1500	s
T_c	$273.15 + 30$	K
T_e	$273.15 + 12$	K
$T_{f,ads}$	$273.15 + 30$	K
$T_{f,reg}$	$273.15 + 200$	K
t_{reg}	$0.91 \times t_{ads}$	s
t_{SG}	12	-
v_{HTF}	0.05	m.s^{-1}
ΔH_{ads}	2.693×10^6	J.kg^{-1}
ε	0.4	-
ρ_m	2700	Kg.m-^{3}
ρ_s	2561	Kg.m-^{3}
σ_s	0.002	m
σ_{tube}	0.001	m

The three dimensional models' results are compared to the high spatial resolution distributed-parameter model results, these used as reference. The criterion for the selection of the spatial resolution of the reference model was to increase the resolution and compare the results to the previous ones, stopping the process when deviations smaller than 0.5% were achieved. This process was carried out for the radial and longitudinal directions using the standard parameters. The selected resolution for the reference model is $\Delta r = 4 \times 10^{-5}\, m$ and $\Delta z = 2.08 \times 10^{-2}\, m$, for the radial and longitudinal directions respectively. The spatial resolution for the 2D model was chosen guaranteeing deviations relative to the reference lower than 1% for both directions using the standard parameters, which correspond to $\Delta r = 5 \times 10^{-5}\, m$ and $\Delta z = 8.33 \times 10^{-2}\, m$. For the 1D model the same radial resolution as for the 2D model was selected. The simulations were carried out for three different HTF velocities. The selected velocities might seem low but they were selected in order to achieve useful temperature increases inside the tubes during the adsorption phase. The calculation time was also measured in order to access the computational cost of

each dimensional model. The COP and SHP values, as well as the deviations relatively to the reference model, and the calculation times are presented in In order to calculate the computational times the function “tic…toc” from MATLAB R2017b (Massachusetts, USA) was used.

Table 2. For this purpose, the reference model is considered as the ‘exact’ solution. In order to calculate the computational times the function “tic…toc” from MATLAB R2017b (Massachusetts, USA) was used.

Table 2 – Results comparison for the different dimensional models using constant parameters.

Model	v_{HTF} ($m.s^{-1}$)	COP	SHP ($W.kg^{-1}$)	$t_{calc.}$ (min)	Φ_{COP} (%)	Φ_{SHP} (%)
Reference	0.050	1.582	217.97	534.00	-	-
2D		1.583	219.94	21.30	0.04	0.90
1D		1.588	219.64	0.15	0.36	0.77
0D		1.608	262.07	0.01	1.61	20.23
Reference	0.025	1.579	209.01	529.90	-	-
2D		1.580	211.46	23.68	0.06	1.17
1D		1.588	219.64	1.67	0.54	5.09
0D		1.608	262.07	0.02	1.79	25.39
Reference	0.010	1.567	183.93	580.55	-	-
2D		1.570	187.63	30.82	0.19	2.01
1D		1.588	219.64	0.15	1.31	19.41
0D		1.608	262.07	0.02	2.56	42.48

2D – Two-dimensional distributed-parameter
1D – One-dimensional distributed-parameter
0D – Lumped-parameter
Φ – Deviation relatively to the reference
$t_{calc.}$ – Calculation time

By analyzing In order to calculate the computational times the function “tic…toc” from MATLAB R2017b (Massachusetts, USA) was used.

Table 2, it is noticeable that for smaller HTF velocities the deviations relative to the reference increase. For the lumped-parameter model it can be concluded that it is not suitable to describe the adsorber’s dynamics since it overestimates the SHP value by more than 20%. Consequently, the lumped-parameter model will not be used for the upcoming analyses. However, it can be a very interesting option to instantaneously provide a first prediction for the system’s performance. The lumped-parameter model predicts the system’s maximum performance since it is able to obtain the maximum and minimum uptake values. However, being a 0D space model, the temperature and pressure changes along the materials are assumed to occur uniformly and the predicted pre-heating and pre-cooling

duration are too low, resulting in cycle times lower than reality, which lead to an overestimation of SHP. The 1D distributed-parameter model can be used for higher HTF velocities, providing good accuracy. As the HTF velocity lowers, the accuracy of the 1D model worsens due to the increase of the temperature differences along the tube length and the adsorbent, which are not taken into account by the model. Meanwhile, the 2D distributed-parameter model proved to require a reasonable computational effort. On the other hand, the high computational effort required by the 2D reference model is not justified, since the improvement on the results' accuracy is irrelevant.

3.2. Metal-adsorbent interface heat transfer coefficient

The heat transfer coefficient at the metal-adsorbent interface has a strong associated uncertainty. Values in the range 100-1000 $W.K^{-1}.m^{-2}$ can be achieved from the literature, depending on the coating technique among other factors. Given this uncertainty, the 1D and 2D models' results were compared using different metal-adsorbent heat transfer coefficients, which are represented in Fig. 4.

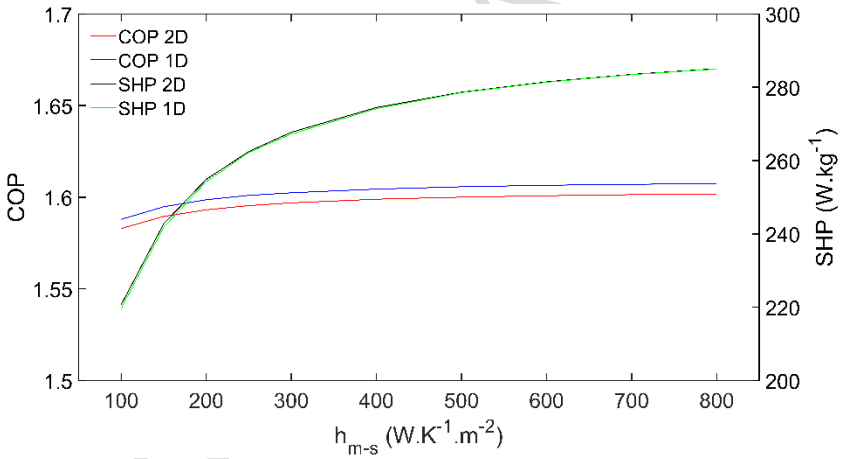

Fig. 4 – COP and SHP as function of the metal-adsorbent heat transfer coefficient obtained with the 1D and 2D models.

These results prove that the 1D model can be used to evaluate the effect of the metal-adsorbent heat transfer coefficient on the performance parameters, since the difference between its predictions and the 2D model's is insignificant. Furthermore, the COP is not significantly affected by this heat transfer coefficient whereas the SHP shows significant variations. Even though the SHP increases with the heat transfer coefficient, this increase fades for heat transfer coefficients higher than 400 $W.K^{-1}.m^{-2}$.

3.3. Adsorber tube length

After performing a first analysis to the considered dimensional models, which resulted in ruling out the lumped-parameter model, the two distributed-parameter models' results were analyzed for different tube lengths. Thus, a comparison between the 1D and 2D models' results for different tube lengths was carried out. For comparison purposes, the 2D model results were taken as the best results, since the reference model would require enormous computational effort, which was found unnecessary. Fig. 5 shows the deviations in COP and SHP obtained when using the 1D model.

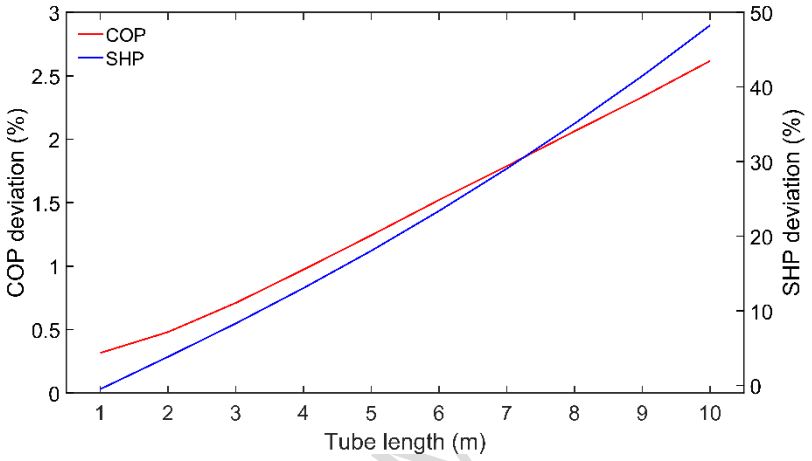

Fig. 5 – COP and SHP deviations as function of the tube length.

The COP is slightly over-predicted by the 1D model being its deviation of ≈2.5% for a 10 m long tube. Thus, the 1D model is a reliable tool to predict the COP, even for long tubes where the temperature changes along the tube's length are significant. On the other hand, the SHP deviation is too high to be despised since it surpasses the 10% mark if a tube longer than 3 m is used. As depicted in Fig. 5, for a 10 m long tube the SHP deviation is over-predicted by approximately one-half of its most accurate value. Therefore, the 1D model can provide accurate predictions if the tube length is not too high; however, it cannot be relied on for longer tubes, where significant temperature variation along the length of the tube occur. Thus, in the following sections the analyses will only contemplate the 2D model.

3.4. Heat transfer fluid velocity

A resolution analysis for the 2D model has been performed in order to evaluate the minimal spatial resolution needed for the desired deviation relative to its high-resolution version, which has been used as reference on the previous sections. The simulations were conducted for different HTF velocities, and the

deviations of the COP and SHP values were investigated for different spatial resolutions. Fig. 6 and Fig. 7 show the deviations for the COP and the SHP, respectively, caused by lowering the resolution of the model in both radial and longitudinal directions. In Figs. 6 and 7, the deviations of the 2D model results relative to the reference results are plotted against the HTF velocity and the radial and longitudinal resolutions, v_{HTF}, Δr and Δz, respectively.

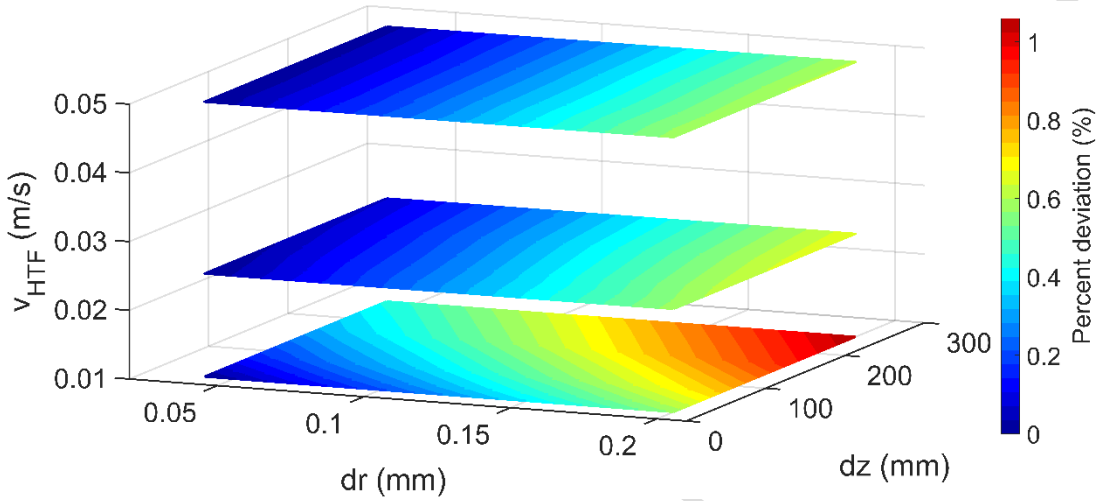

Fig. 6 – COP percent deviation as function of the axial and radial direction resolutions, respectively *Δz* and *Δr*, and the heat transfer fluid velocity.

For higher HTF velocities the COP deviations are affected mainly by the radial resolution; however, for lower HTF velocities the longitudinal resolution also begins to cause COP deviations. Although, even for the smallest HTF velocity, the COP deviations caused by using a lower resolution are small.

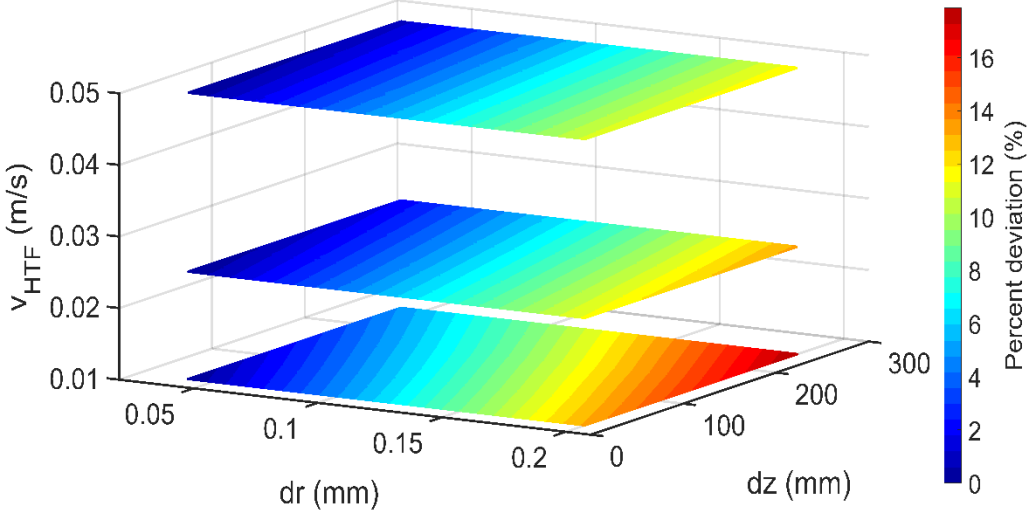

Fig. 7 - SHP percent deviation as function of the axial and radial direction resolutions, respectively *Δz* and *Δr*, and the heat transfer fluid velocity.

On the other hand, the SHP deviations caused by lowering the resolution are significant. The radial resolution strongly affects the accuracy of the SHP predictions for all HTF velocities tested. The influence of the longitudinal resolution on the accuracy increases as the HTF's velocity decreases, reaching ≈5% for the smallest HTF velocity tested. For the lowest resolution the obtained SHP deviations are 12%, 13% and 18% for the respective HTF velocities of 0.050 m.s^{-1}, 0.025 m.s^{-1} and 0.010 m.s^{-1}. From the analysis it is concluded that a 2D spatial resolution with $\Delta r = 5 \times 10^{-5}\ m$ and $\Delta z = 8.33 \times 10^{-2}\ m$ is enough to guarantee a total SHP deviation of only ≈1% under the worst-case scenario tested (lowest HTF's velocity). It is important to note that there is a difference of 700 min on the calculation time when using the highest and lower spatial resolutions. The difference on the calculation time between the selected best resolution and the highest resolution is of 670 min for the standard parameters. The selected best radial and longitudinal resolution requires much less computational effort, and still provides accurate results.

3.5. Metal mass

Although some studies take into consideration the mass of the adsorber's metal tubes [39–41], this parameter is often disregarded or not mentioned in many studies for the calculation of the resultant heat from an AHP cycle [22–24]. The effects of considering this metal mass on the physical models were evaluated. In order to quantify these effects, the 2D distributed-parameter model was used to simulate the AHP cycle. Simulations were carried out considering the metal tube mass and disregarding it ($m_m = 0$), for different inner tube diameters and for two distinct HTF's velocities. The COP and SHP deviations due to disregarding of the tube's metal mass are presented in Table 3.

Table 3 – Deviations of COP and SHP due to disregarding the tube metal mass.

Inner tube diameter (mm)	HTF velocity = 0.01 m/s		HTF velocity = 0.05 m/s	
	COP deviation	SHP deviation	COP deviation	SHP deviation
5	3.7%	-6.0%	3.4%	-5.3%
10	4.1%	-6.4%	4.0%	-6.1%
20	4.5%	-7.1%	4.5%	-7.0%

By analyzing Table 3 it is concluded that not considering the metal mass has a significant impact on the prediction of the system's performance. The COP is always overestimated whereas the SHP is always underestimated, with the SHP prediction being the most affected. On the other hand, the deviations of

disregarding the tube metal mass are not significantly affected by the HTF velocity. It is thus concluded that the tube's metal mass should not be disregarded unless deviations up to ≈4.5% on the COP and up to ≈7% on the SHP values can be considered acceptable.

4. Conclusions

Analysis of different transient dimensional models describing a coated tube adsorber for an AHP system was carried out. Three different dimensional models were considered and results compared, namely a 0D lumped-parameter model, a 1D distributed-parameter model and a 2D distributed-parameter model. All the analyses reported help on the selection of the dimensional model that must be used for different adsorption heat pump simulations. Furthermore, parametric sensibility was achieved and an evaluation of the deviations that are associated with each dimensional model was performed. Thus, sustained decisions about which dimensional model must be used in order to achieve suitable accuracies for particular applications can be made, taking into account the deviations and the computational costs associated to each dimensional model.

It was concluded that the lumped-parameter model is not suitable to describe the adsorber's dynamics unless a deviation over 20% can be admitted, since the SHP is overestimated. On the other hand, the results show that the lumped model can be used to predict the COP, with deviations up to ≈2% relative to the high-resolution reference model.

The 1D radially distributed parameter model can be used for a very quick prediction of the adsorber's performance coefficients, providing results with insignificant deviations for the COP. Although the 1D model cannot be relied on for lower HTF's velocities, for higher HTF's velocities that result in low temperature differences along the tube length, the 1D model also provides accurate results for the SHP. However, by carrying out tests for longer tube lengths it was found that this model does not provide accurate predictions for the SHP, with deviations up to 50% for a 10 m long tube due to the high temperature variation along the tube length. Information on whether the utilization of a 1D model is suitable or not depending on the tube length is now available.

From the simulations performed with the 2D (radial and longitudinal) distributed-parameter model for different HTF's velocities, it was concluded that the spatial resolutions tested had no significant impact on the COP predictions. Nevertheless, the SHP predictions are significantly influenced by the spatial resolution since deviations up to ≈17% were obtained using the lowest resolution. In addition, it was found that the radial resolution has greater influence on the accuracy of the model than the longitudinal resolution, which only becomes

significant for lower HTF's velocities. Therefore, a spatial resolution of $\Delta r = 5 \times 10^{-5}\, m$ and $\Delta z = 8.33 \times 10^{-2}\, m$ should be used in order to guarantee a total deviation of ≈1% for the SHP value for the worst-case scenario, with the lowest computational cost. It is thus concluded that the 2D distributed-parameter model should be selected if a detailed and accurate description of an AHP system is desired.

Finally, the influence of disregarding the metal mass of the adsorber was investigated. Results show that not accounting for this metal mass leads to significant deviations on the COP and SHP predictions. Deviations up to ≈4.5% for the COP and up to ≈7% for the SHP were obtained due to the disregarding of the metal tube mass.

Acknowledgements

The present study was developed in the scope of the Smart Green Homes Project [POCI-01-0247-FEDER-007678], a co-promotion between Bosch Termotecnologia S.A. and the University of Aveiro. It is financed by Portugal 2020 under the Competitiveness and Internationalization Operational Program, and by the European Regional Development Fund.

The authors acknowledge the Portuguese Foundation for Science and Technology for the financial support provided through project UID/EMS/00481/2013-FCT, and CENTRO-01-0145-FEDER-022083.

References

[1] European Commision. Communication from the commission to the European parliament, the council, the European economic and social committee and the committee of the regions. Brussel: 2016.

[2] Tokarev MM, Gordeeva LG, Grekova AD, Aristov YI. Adsorption cycle “heat from cold” for upgrading the ambient heat: The testing a lab-scale prototype with the composite sorbent CaClBr/silica. Appl Energy 2018;211:136–45.

[3] Dawoud B. On the development of an innovative gas-fired heating appliance based on a zeolite-water adsorption heat pump; System description and seasonal gas utilization efficiency. Appl Therm Eng 2014;72:323–30. doi:10.1016/j.applthermaleng.2014.09.008.

[4] Ramji HR, Leo SL, Abdullah MO. Parametric study and simulation of a heat-driven adsorber for air conditioning system employing activated carbon-methanol working pair. Appl Energy 2014;113:324–33. doi:10.1016/j.apenergy.2013.07.017.

[5] Zhang LZ, Wang L. Performance estimation of an adsorption cooling system for automobile waste heat recovery. Appl Therm Eng 1997. doi:10.1016/S1359-4311(97)00039-2.

[6] Fernandes MS, Brites GJVN, Costa JJ, Gaspar AR, Costa VAF. A thermal energy storage system provided with an adsorption module – Dynamic modeling and viability study. Energy Convers Manag 2016;126:548–60. doi:10.1016/j.enconman.2016.08.032.

[7] Sakoda A, Suzuki M. Fundamental study on solar powered adsorption cooling system. J Chem Eng Japan 1984;17:52–7. doi:10.1252/jcej.17.52.

[8] Sakoda A, Suzuki M. Simultaneous transport of heat and adsorbate in closed type adsorption cooling system utilizing solar heat. J Sol Energy Eng Trans ASME 1986. doi:10.1115/1.3268099.

[9] Sawin JL, Seyboth K, Sverrisson F. Renewables 2017: Global status report. 2017.

[10] Ulku S. Adsorption heat pumps. J Heat Recover Syst 1986;6:277–84. doi:10.1016/0198-7593(86)90113-X.

[11] Freni A, Dawoud B, Bonaccorsi L, Chmielewski S, Frazzica A, Calabrese L, et al. Characterization of zeolite-based coatings for adsorption heat pumps. Springer; 2015.

[12] Dias JMS, Costa VAF. Adsorption heat pumps for heating applications: A review of current state, literature gaps and development challenges. Renew Sustain Energy Rev 2018;98:317–27. doi:10.1016/J.RSER.2018.09.026.

[13] Pesaran A, Lee H, Hwang Y, Radermacher R, Chun HH. Review article: Numerical simulation of adsorption heat pumps. Energy 2016;100:310–20. doi:10.1016/j.energy.2016.01.103.

[14] Sircar S. Linear-driving-force model for non-isothermal gas adsorption kinetics. J Chem Soc Faraday Trans 1 Phys Chem Condens Phases 1983;79:785. doi:10.1039/f19837900785.

[15] Rivero-Pacho AM, Critoph RE, Metcalf SJ. Modelling and development of a generator for a domestic gas-fired carbon-ammonia adsorption heat pump. Renew Energy 2017;110:180–5. doi:10.1016/j.renene.2017.03.089.

[16] Rezk ARM, Al-Dadah RK. Physical and operating conditions effects on silica gel/water adsorption chiller performance. Appl Energy 2012;89:142–9.

[17] Frazzica A, Füldner G, Sapienza A, Freni A, Schnabel L. Experimental and theoretical analysis of the kinetic performance of an adsorbent coating composition for use in adsorption chillers and heat pumps. Appl Therm Eng 2014;73:1020–9. doi:10.1016/j.applthermaleng.2014.09.004.

[18] Freni A, Bonaccorsi L, Calabrese L, Caprì A, Frazzica A, Sapienza A. SAPO-34 coated adsorbent heat exchanger for adsorption chillers. Appl Therm Eng 2015;82:1–7. doi:10.1016/j.applthermaleng.2015.02.052.

[19] Wittstadt U, Füldner G, Laurenz E, Warlo A, Große A, Herrmann R, et al. A novel adsorption module with fiber heat exchangers: Performance analysis based on driving temperature differences. Renew Energy 2017;110:154–61. doi:10.1016/j.renene.2016.08.061.

[20] Calabrese L, Brancato V, Bonaccorsi L, Frazzica A, Caprì A, Freni A, et al. Development and characterization of silane-zeolite adsorbent coatings for adsorption heat pump applications. Appl Therm Eng 2017;116:364–71. doi:10.1016/j.applthermaleng.2017.01.112.

[21] Fernandes MS, Brites GJVN, Costa JJ, Gaspar AR, Costa VAF. Modeling and parametric analysis of an adsorber unit for thermal energy storage. Energy 2016;102:83–94. doi:10.1016/j.energy.2016.02.014.

[22] Zhang LZ, Wang L. Effects of coupled heat and mass transfers in adsorbent on the performance of a waste heat adsorption cooling unit. Appl Therm Eng 1999;19:195–215. doi:10.1016/S1359-4311(98)00023-4.

[23] Restuccia G, Freni A, Maggio G. A zeolite-coated bed for air conditioning adsorption systems: Parametric study of heat and mass transfer by dynamic simulation. Appl. Therm. Eng., vol. 22, 2002, p. 619–30. doi:10.1016/S1359-4311(01)00114-4.

[24] Pinheiro JM, Salústio S, Rocha J, Valente AA, Silva CM. Analysis of equilibrium and kinetic parameters of water adsorption heating systems for different porous metal/metalloid oxide adsorbents. Appl Therm Eng 2016;100:215–26. doi:10.1016/j.applthermaleng.2016.01.142.

[25] Ng KC, Chua HT, Chung CY, Loke CH, Kashiwagi T, Akisawa A, et al. Experimental investigation of the silica gel-water adsorption isotherm characteristics. Appl Therm Eng 2001. doi:10.1016/S1359-4311(01)00039-4.

[26] Di J, Wu JY, Xia ZZ, Wang RZ. Theoretical and experimental study on characteristics of a novel silica gel-water chiller under the conditions of variable heat source temperature. Int J Refrig 2007. doi:10.1016/j.ijrefrig.2006.07.022.

[27] Chua HT, Ng KC, Chakraborty A, Oo NM, Othman MA. Adsorption characteristics of silica gel + water systems. J Chem Eng Data 2002. doi:10.1021/je0255067.

[28] Wang D, Zhang J, Yang Q, Li N, Sumathy K. Study of adsorption characteristics in silica gel-water adsorption refrigeration. Appl Energy 2014. doi:10.1016/j.apenergy.2013.08.011.

[29] Wu JY, Li S. Study on cyclic characteristics of silica gel-water adsorption cooling system driven by variable heat source. Energy 2009. doi:10.1016/j.energy.2009.08.003.

[30] Boman DB, Hoysall DC, Pahinkar DG, Ponkala MJ, Garimella S. Screening of working pairs for adsorption heat pumps based on thermodynamic and transport characteristics. Appl Therm Eng 2017;123:422–34. doi:10.1016/j.applthermaleng.2017.04.153.

[31] Wilkes JO, Birmingham SG. Fluid Mechanics for Chemical Engineers with Microfluidics and CFD. Pearson Education; 2006.

[32] Aristov YI. Optimal adsorbent for adsorptive heat transformers: Dynamic considerations. Int J Refrig 2009. doi:10.1016/j.ijrefrig.2009.01.022.

[33] Do Duong D. Adsorption Analysis: Equilibria And Kinetics (With Cd Containing Computer Matlab Programs). vol. 2. World Scientific; 1998.

[34] Bergman TL, Lavigne AS, Incropera FP, Dewitt DP. Fundamentals of Heat and Mass Transfer. John Wiley & Sons; 2011. doi:10.1016/j.applthermaleng.2011.03.022.

[35] Gnielinski V. New Equations for Heat and Mass Transfer in Turbulent Pipe and Channel Flow. Int Chem Eng 1976.

[36] Petukhov BS. Heat Transfer and Friction in Turbulent Pipe Flow with Variable Physical Properties. Adv Heat Transf 1970. doi:10.1016/S0065-2717(08)70153-9.

[37] Chakraborty A, Saha BB, Aristov YI. Dynamic behaviors of adsorption chiller: Effects of the silica gel grain size and layers. Energy 2014. doi:10.1016/j.energy.2014.10.015.

[38] Sun B, Chakraborty A. Thermodynamic frameworks of adsorption kinetics

modeling: Dynamic water uptakes on silica gel for adsorption cooling applications. Energy 2015. doi:10.1016/j.energy.2015.02.101.

[39] Kowsari MM, Niazmand H, Tokarev MM. Bed configuration effects on the finned flat-tube adsorption heat exchanger performance: Numerical modeling and experimental validation. Appl Energy 2017. doi:10.1016/j.apenergy.2017.11.019.

[40] Freni A, Maggio G, Sapienza A, Frazzica A, Restuccia G, Vasta S. Comparative analysis of promising adsorbent/adsorbate pairs for adsorptive heat pumping, air conditioning and refrigeration. Appl Therm Eng 2016;104:85–95. doi:10.1016/j.applthermaleng.2016.05.036.

[41] Sapienza A, Gullì G, Calabrese L, Palomba V, Frazzica A, Brancato V, et al. An innovative adsorptive chiller prototype based on 3 hybrid coated/granular adsorbers. Appl Energy 2016;179:929–38. doi:10.1016/j.apenergy.2016.07.056.

Highlights

- Development and discussion of three different dimensional models for AHPs.
- Comparisons between different dimensional models.
- Influence of certain parameters on the dimensional models results' accuracy.
- Selection of the best spatial resolution for the different dimensional models.
- Deviations caused by disregarding the adsorber metal tubes' mass.